AD 297 434

NOTICE: When government or other drawings, specifications or other data are used for any purpose other than in connection with a definitely related government procurement operation, the U. S. Government thereby incurs no responsibility, nor any obligation whatsoever; and the fact that the Government may have formulated, furnished, or in any way supplied the said drawings, specifications, or other data is not to be regarded by implication or otherwise as in any manner licensing the holder or any other person or corporation, or conveying any rights or permission to manufacture, use or sell any patented invention that may in any way be related thereto.

RADC TDR-63-49
AF 61(052) 552
15 Dec. 1962

SUMMARY REPORT

INTERACTION BETWEEN MICROWAVES AND PLASMAS IN GAS DISCHARGES AND SEMICONDUCTORS

B. AGDUR

ROYAL INSTITUTE OF
TECHNOLOGY
STOCKHOLM, SWEDEN
MICROWAVE DEPARTMENT

The research reported in this document has been sponsored by, or in part by, the Rome Air Development Centre of the Air Force Systems Command through the European Office, Aerospace Research, United States Air Force.

ABSTRACT

This summary report describes theoretical and experimental investigations of wave propagation in cylindrical plasma columns and plasma resonance phenomenon in semiconductors.

CONTENTS

1. INTRODUCTION

The theoretical work in the field of gas discharge plasma amplifiers has been concentrated on studies on wave propagation along plasma columns and on the problem of coupling of waves in such systems. The experimental work has included studies of different plasma systems for plasma amplifiers and studies of wave propagation in various regions of plasma density and magnetic field strength. The work on semiconductor plasmas during this period has been concentrated on a study of plasma resonance phenomenon in such plasmas. It may also be mentioned that similar investigations has been made on metal plasmas[1].

2. GASEOUS DISCHARGE PLASMAS

2.1. Modes in anisotropic plasma waveguides

The purpose has been to investigate the properties of a certain class of modes which can propagate in the plasma-waveguide shown in Fig. 1. The waveguide consists of a circularly cylindrical tube containing a central homogeneous plasma column. The investigation has been confined to the circularly symmetric modes existing in region 4 of Fig. 2. For given values of the parameters ω_p/ω and ω_c/ω there are infinitely many symmetric modes that can propagate in the guide. Only the first radial mode will be considered here.

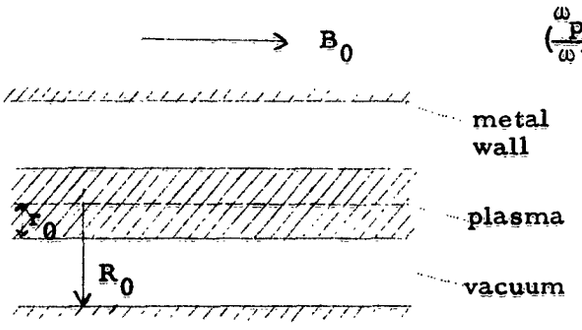

Fig. 1.

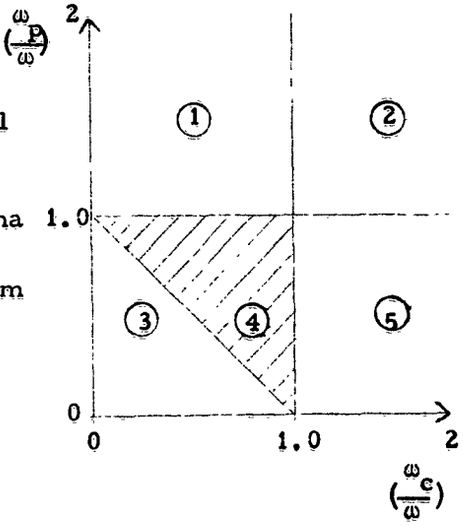

Fig. 2.

Dispersion curves and field distribution has been calculated using the exact equations given in[2]. In contrast to earlier investigations of the same system[3], our results are valid for waves having arbitrary phase velocities.

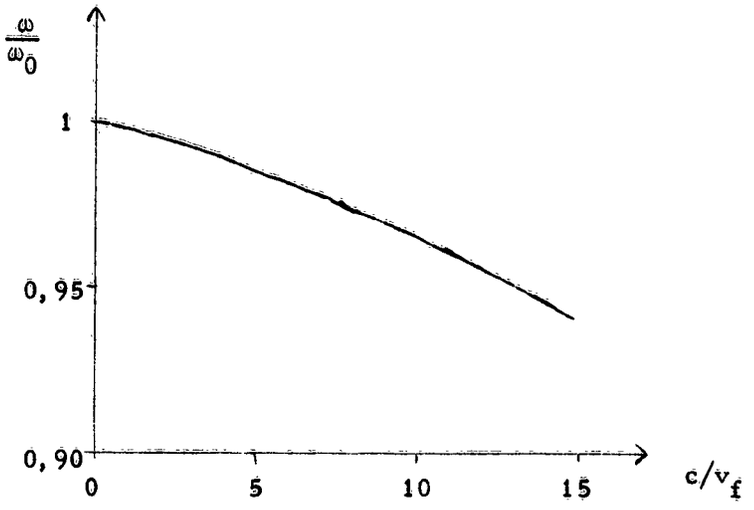

Fig. 3.

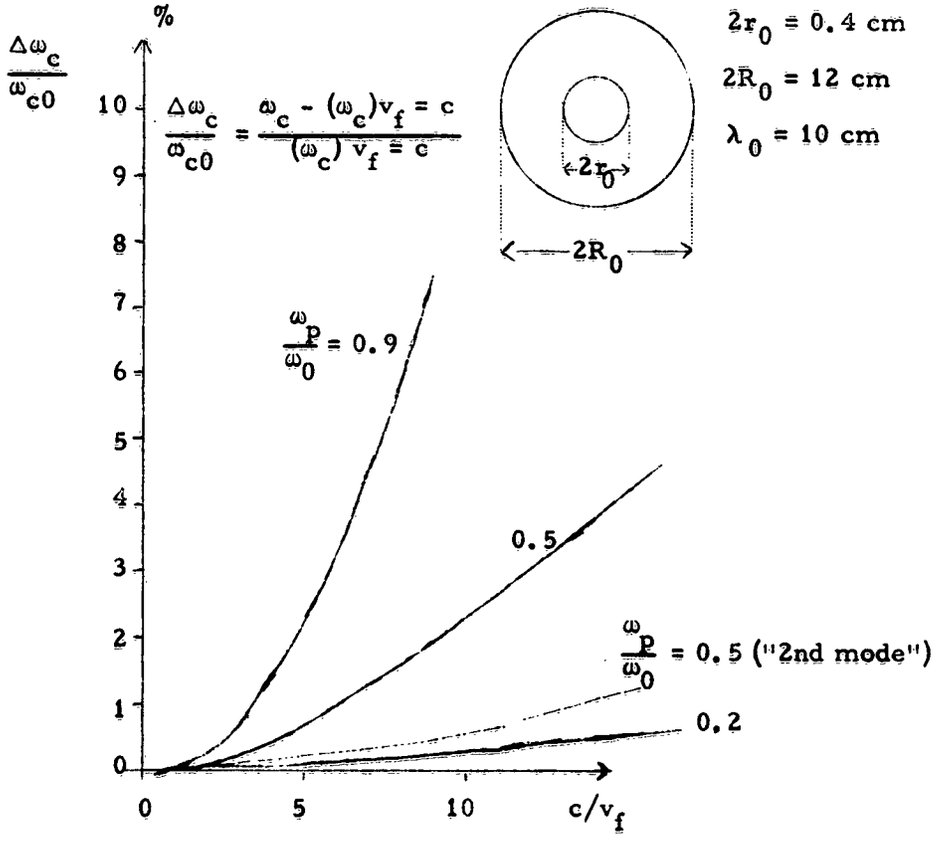

Fig. 4.

Fig. 3 shows a typical dispersion curve. The phase velocity, v_f, is increasing with increasing frequency and the wave is therefore a backward wave having the phase velocity and the group velocity in opposite directions. As shown by Fig. 4 the phase velocity is extremely sensitive to variations in the magnetic field. In an experimental investigation of these modes, it would therefore be necessary to have a very homogeneous magnetic field.

The variation in a crossection of the axial electric field, E_z, the radial electric field, E_r, and the azimuthal magnetic field, H_φ, is shown in Fig. 6. for three different sets of parameters. The fields inside the plasma column are much stronger than outside. The ratio between the power that propagates in the region outside the plasma, P_u, to the total power propagating in the waveguide, P_z, is shown in Fig. 5. The results obtained by slow wave approximation are given for comparison.

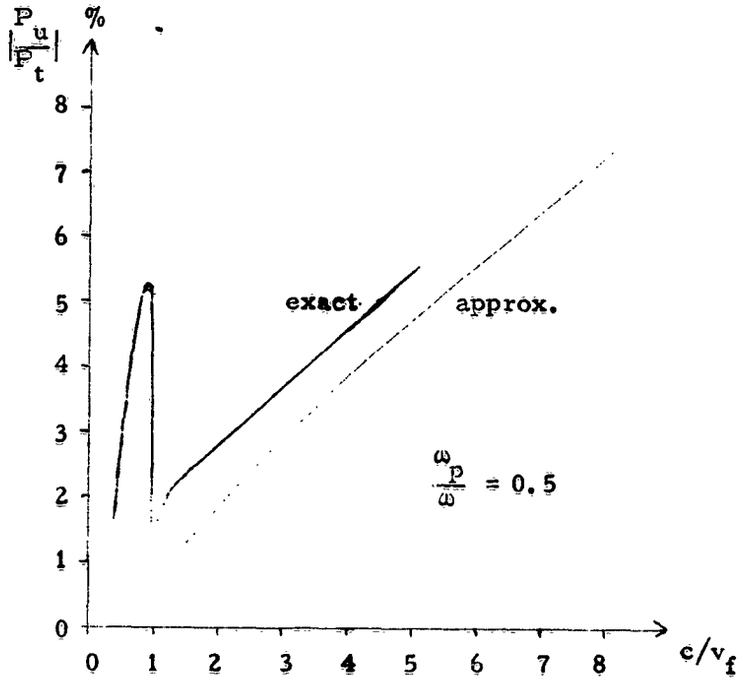

Fig. 5.

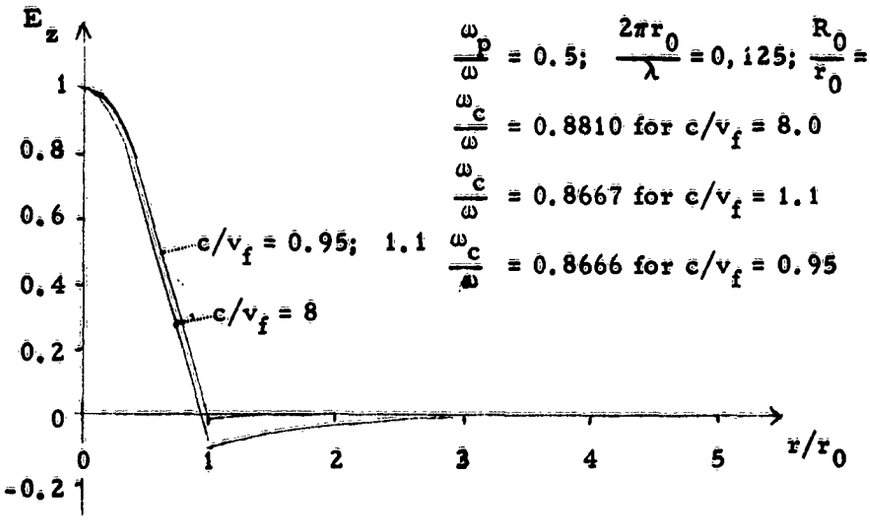
E_z
1
0.8
0.6
0.4
0.2
0
-0.2
0
1
2
3
4
5
r/r_0
$c/v_f = 0.95;\ 1.1$
$c/v_f = 8$
$\frac{\omega_p}{\omega} = 0.5;\ \frac{2\pi r_0}{\lambda} = 0,125;\ \frac{R_0}{r_0} = 30$
$\frac{\omega_c}{\omega} = 0.8810$ for $c/v_f = 8.0$
$\frac{\omega_c}{\omega} = 0.8667$ for $c/v_f = 1.1$
$\frac{\omega_c}{\omega} = 0.8666$ for $c/v_f = 0.95$

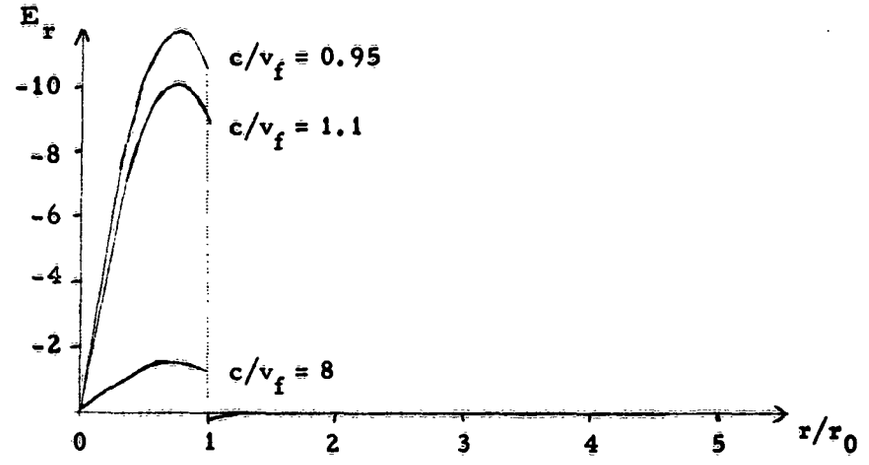
E_r
-10
-8
-6
-4
-2
0
1
2
3
4
5
r/r_0
$c/v_f = 0.95$
$c/v_f = 1.1$
$c/v_f = 8$

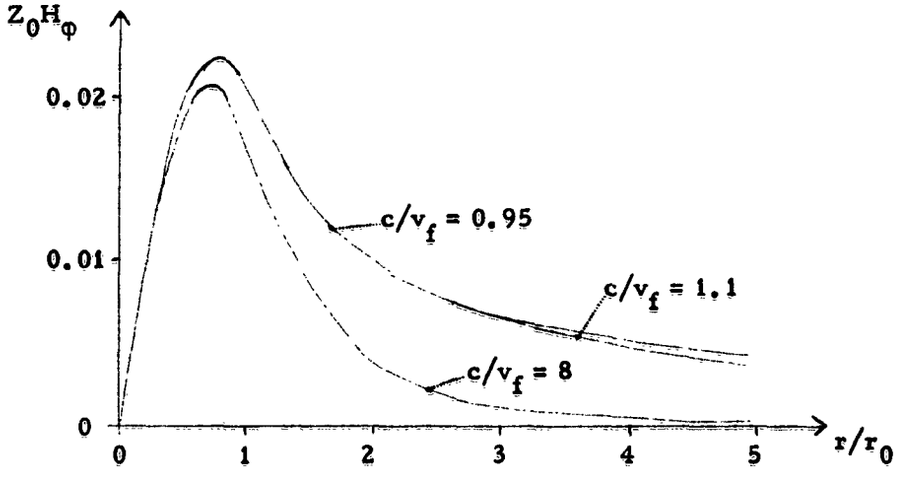
Z_0H_φ
0.02
0.01
0
0
1
2
3
4
5
r/r_0
$c/v_f = 0.95$
$c/v_f = 1.1$
$c/v_f = 8$

Fig. 6.

2.1. Dispersion characteristics for plasma modes in isotropic plasma waveguides

The dispersion curves for some of the modes in a waveguide partially filled with a homogeneous, lossless plasma have been calculated. It is found that, under certain conditions, backward waves can exist even in the absence of a static magnetic field. The dispersion curves then have singular points where $\frac{\partial\omega}{\partial\beta}$ goes through zero and changes sign.

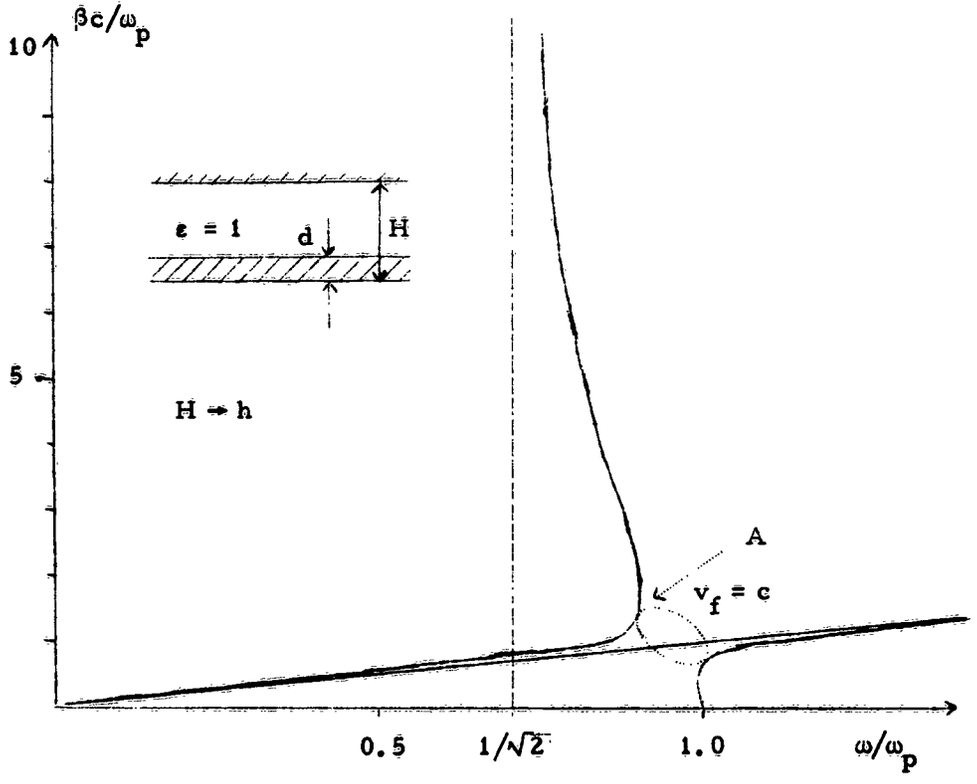

Fig. 7.

The dispersion equation for the plane parallel lossless plasma waveguide system shown in Fig. 7 can be written in the following form

$$\frac{k_{II}}{\varepsilon_{II}} \operatorname{tgh}(k_{II}d) = -k_I \operatorname{tgh}[k_I(h-d)]$$

where a field variation $\exp[j(\omega t - \beta z)]$ is assumed and

$$\varepsilon_{II} = \left[1 - \left(\frac{\omega_p}{\omega}\right)^2\right]$$

$$k_I = \sqrt{\beta^2 - \left(\frac{\omega}{c}\right)^2}$$

$$k_{II} = \sqrt{\beta^2 - \varepsilon_{II}\left(\frac{\omega}{c}\right)^2}$$

d = thickness of plasma sheath

h = distance between the metal walls

Fig. 7 shows characteristic features of the β, ω-diagram for real values of β with $d/h = 0.05$ and $\omega_p d/c = 0.1$.

A Taylor series expansion of the characteristic equation around a point where $\partial\omega/\partial\beta$ is zero shows that the curve must have four branches starting in such a point, two of which have complex conjugate values and correspond to cut-off solutions. At point A in Fig. 7 these complex solutions are indicated by the dashed curves which connect two of the branches for propagating modes. If losses are introduced the branchpoints disappear and there is a unique transition from the propagating branches of the curves to the cut-off branches.

In addition computations of dispersion curves for modes with one azimuthal variation have been made for circularly cylindrical systems as shown in Fig. 8. This dispersion curve also has branches where $\partial\omega/\partial\beta$ is negativ. Backward waves do also exist on a plasma column which is not surrounded by any metallic waveguide.

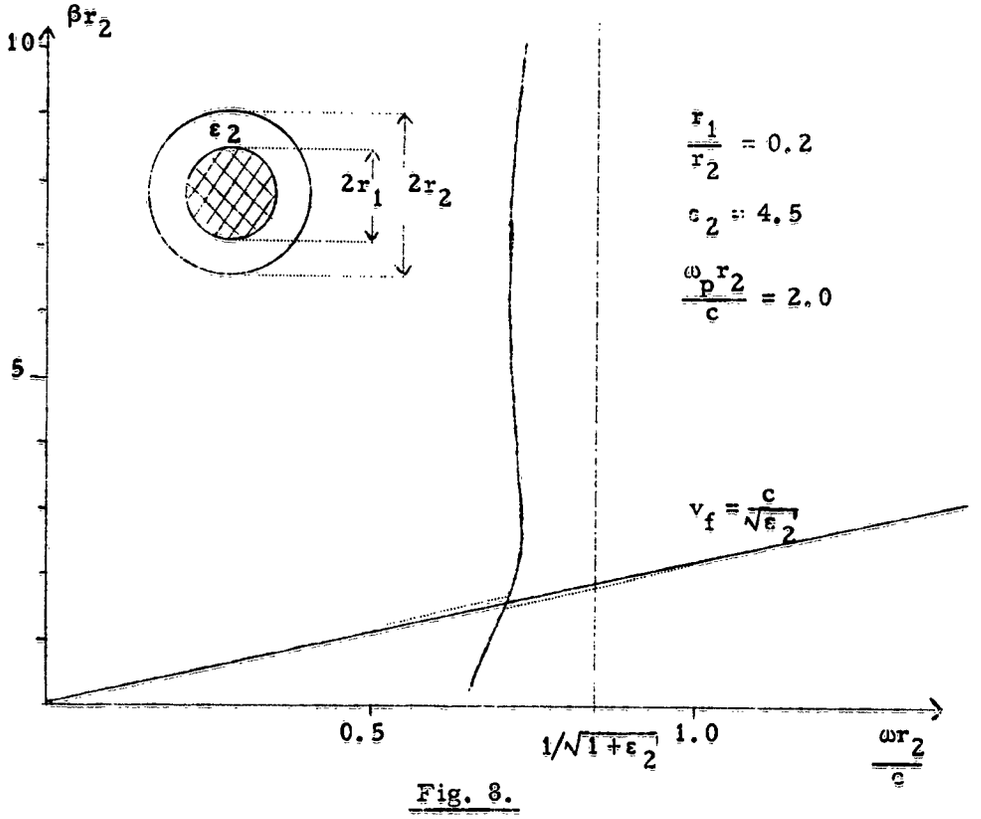

Fig. 8.

2.3 Discontinuity problems in plasma waveguides

To investigate how one can couple microwave energy from ordinary waveguides to plasma waveguides, two systems have been considered.

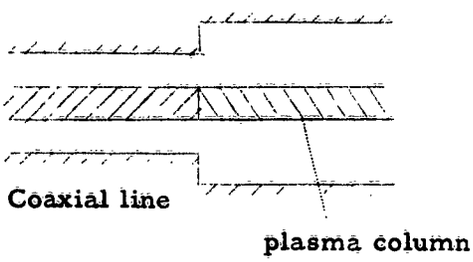

Fig. 9.

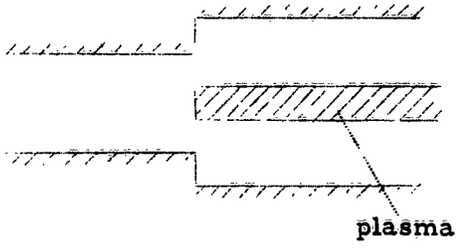

Fig. 10.

In the first system a coaxial line is connected to a circularly cylindrical waveguide containing a plasma column. It is assumed that the plasma is cool, collisionless and homogeneous, and that no static magnetic field is present. The dimensions of the coaxial-line are such that only the TEM-mode can propagate. In the plasma waveguide the plasma density and the dimensions are such that, of the circularly symmetric modes, only the slow "plasma"-mode is above cut-off. Because of the discontinuity an incident TEM-mode in the coaxial line excites all possible symmetric modes in the two waveguide sections, but far away from the junction only the two modes just mentioned are of importance. It is desired to know how much of the energy in the incident wave that is transmitted into the plasma waveguide.

The second system (Fig. 10) consists of a circularly cylindrical waveguide connected to a similar waveguide containing a plasma column. Of the circularly symmetric modes only the TM_{01}-mode is above cut-off in the empty waveguide and only the slow "plasma"-mode in the plasma-waveguide. The transmission is studied when a TM-mode is incident in the empty waveguide.

The transverse electric and magnetic fields in the empty waveguide (or coaxial-line) can be written

$$E_r^I = a_1(e^{\gamma_1 z} + R_1 e^{\gamma_1 z})\Phi_1 + \sum_{n=2}^{\infty} a_n \Phi_n e^{\gamma_n z}; \quad E_\varphi = 0$$

$$H_\varphi^{II} = a_1 Y_1(e^{-\gamma_1 z} - R_1 e^{\gamma_1 z})\Phi_1 - \sum_{n=2}^{\infty} a_n Y_n \Phi_n e^{\gamma_n z}$$

In the plasma-waveguide the fields can be expressed in the following way

$$E_r^{II} = \sum_{m=1}^{\infty} b_m \psi_m e^{-\gamma_m z}$$

$$H_\varphi^{II} = \sum_{m=1}^{\infty} b_m Y_m \psi_m e^{-\gamma_m z}$$

where $\phi_n = \phi_n(r)$ and $\psi_m = \psi_m(r)$ are the complete orthogonal sets of eigenfunctions for E_r in the two waveguides, γ_n and γ_m are the corresponding propagation constants, R_1 is the reflection coefficient for the incident mode in the empty waveguides, $Y_n = j\omega\varepsilon_0/\gamma_n$ and $Y_m = j\omega\varepsilon(r)\varepsilon_0/\gamma_n$. Using the boundary conditions $E_r^I = E_r^{II}$, $H_\varphi^I = H_\varphi^{II}$ we can form the following variational expression:

$$\frac{1 - R_1}{1 + R_1} = \frac{\sum_{n=2}^{\infty}\{\int_a^b E'(r)\, Y_n \phi_n\, r\, dr\}^2 + \sum_{m=1}^{\infty}\{E'(r)\, Y_m \psi_m\, r\, dr\}^2}{Y_1^2\ \{\int_a^b E'(r)\, \phi_1(r)\, r\, dr\}^2}$$

which is stationary for small arbitrary variations in the electric field distribution, $E'(r)$, about its exact value. This expression is presently used to compute the reflection coefficient R_1 by using suitable approximations for the functions $E'(r)$.

2.4. Experiments on slow wave plasma modes

The propagation of slow waves in a circular waveguide partially filled with plasma was investigated experimentally. The plasma used in this experiment was the positive column of an arc discharge in mercury vapor. The mercury gas pressure was estimated from temperature measurements to be of the order of 10^{-3} mm Hg. The plasma density could be varied by controlling the discharge current. Both 50 c/s sine wave and sawtooth sweeping currents were used. The chief difficulties were that the plasma density drifted and that the column tended to oscillate at frequencies between 10 and 100 kc. To avoid these difficulties the plasma could be operated in "after-glow".

The measurements were carried out at frequencies in the range from 1000 to 3000 Mc. A schematic diagram of the apparatus used to investigate the properties of various modes is shown in Fig. 11. The r.f. signal could be coupled into the plasma waveguide in three different ways: 1) by a cavity operating in TM_{010}-mode; 2) by the discharge anode; 3) by a loop.

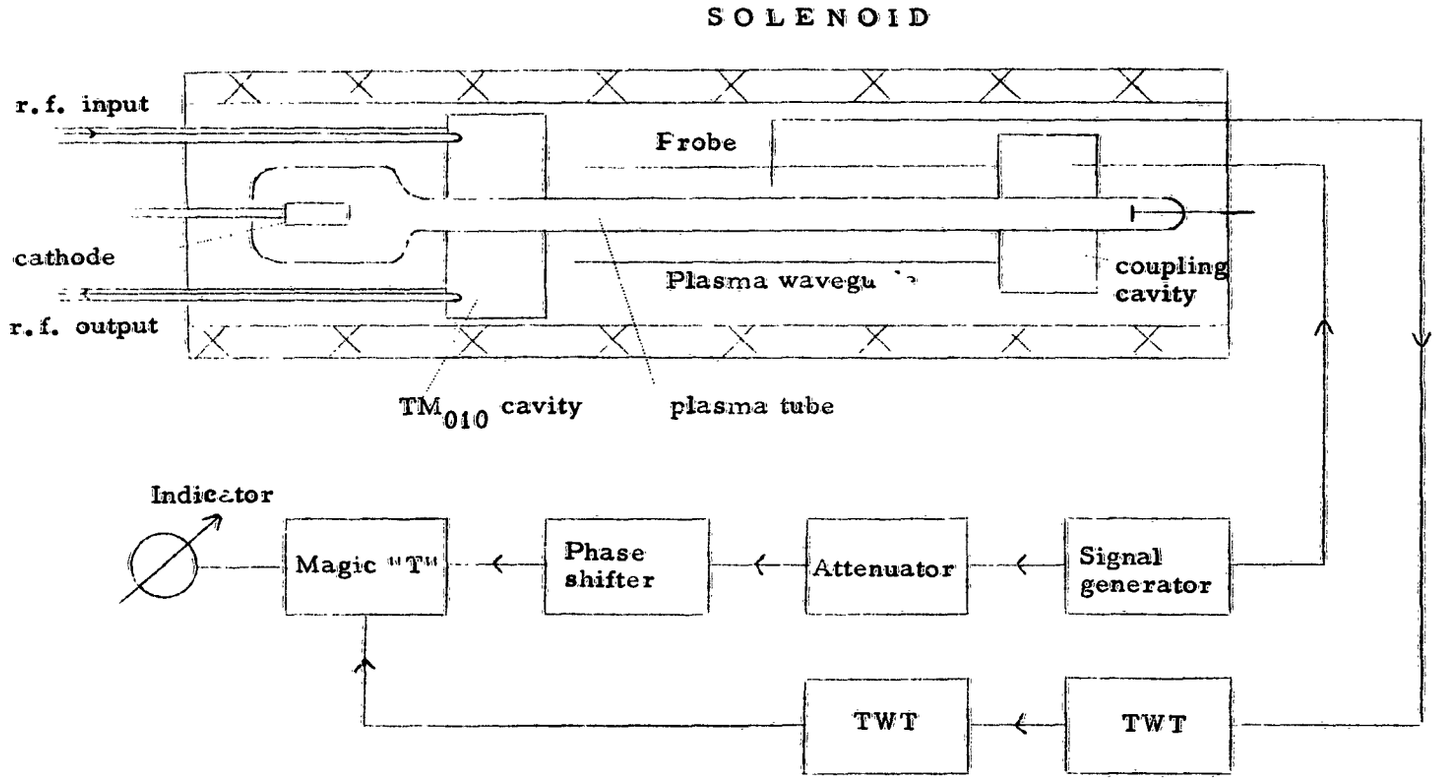
SOLENOID
r.f. input
Probe
cathode
Plasma waveg
coupling cavity
r.f. output
TM010 cavity
plasma tube
Indicator
Magic "T"
Phase shifter
Attenuator
Signal generator
TWT
TWT

Fig. 11.

The fields in the plasma waveguide were detected by means of a moveable probe. The wavelength was measured in two different ways. The first method was to measure the standing waves along the plasma wave-guide. When the losses were rather high (and the wave-length short) the wave-length was measured by means of an interferometer. The electron density was measured simultaneously by means of the microwave cavity method.

Propagation of slow waves was investigated experimentally in the region $0 < (\frac{\omega_p}{\omega})^2 < 6$ and $0 < (\frac{c}{\omega})^2 < 1$ (Fig. 2). When the plasma parameters are adjusted so that we are in region (1), see Fig. 2, there is generally a good agreement between theory and experiment. It is, however, very interesting to notice that it has been impossible to detect any waves in region 4. The theory predicts propagating modes in this region and a study of the coupling mechanism shows that it should be possible to excite these waves.

In another experiment we have studied the propagation of the dipole-mode in a circular waveguide, partially filled with a plasma and with zero static magnetic field. Special attention was given to the negative dispersion of this mode.

The generation and the control of the plasma are the same as described in the previous experiment. Low frequency instabilities and drift in the electron density made it important to choose proper values of parameters such as pressure, dimensions and density.

The dispersion curve can be plotted if the wave-length is measured for different frequencies. As the dipole-wave is strongly attenuated, the interferrometer method had to be used when measuring the wave-length. In order to exite the dipol-mode, the r.f. signal was coupled unsymmetrically to the waveguide, by means of two loops.

The measurements were performed in the frequency-range 1000-2000 Mc and the plasma frequency was about 2500 Mc. The experimental results is shown in Fig. 12. The curve shows a negative dispersion in agreement with the theory.

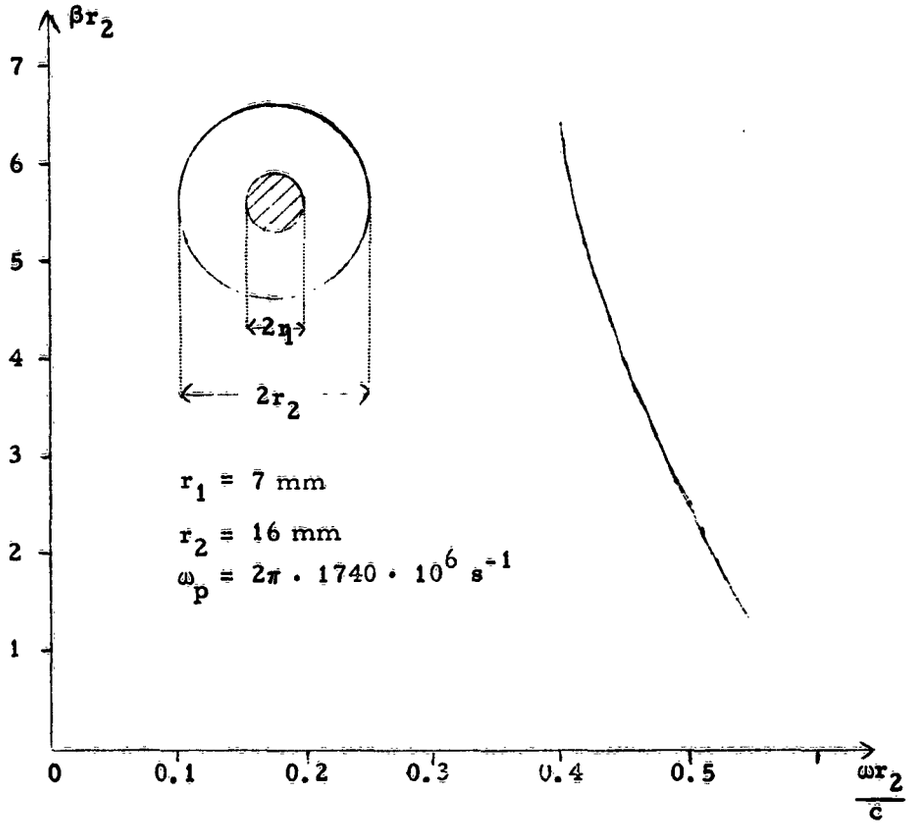

Fig. 12.

2.5 Methods of creating a highly ionized cesium plasma

It is known that a highly ionized quiescent plasma can be generated by means of resonance ionization of cesium. In order to get equilibrium between the ion generation and electron emission from the metal surface, it is necessary to heat the metal to a very high temperature. We are using a tantalum disc to obtain the plasma. It is also important to create this high temperature on the disc without any surrounding disturbing electric or magnetic fields. One method of doing this is to heat the disc by means of an electron beam. This is, however, very complicated and we have therefore been investigating three other methods.

The first method consists of heating with a concentrated light-beam. We use a Xenon high pressure discharge lamp, which has a temperature of 6000°C. The lamp is placed in one focus of an ellipsoidal mirror while the tantalum disc is placed in the other focus. The desired temperature - about 2000°C - is easily obtained with this method. We think that this method is a very useful one to obtain very high temperatures. However, in this special case we met some difficulties in constructing a tube which could stand the heating from light radiation. It was necessary to make the tube out of quartz, which was inconvenient in our case. The device is shown in Fig. 13.

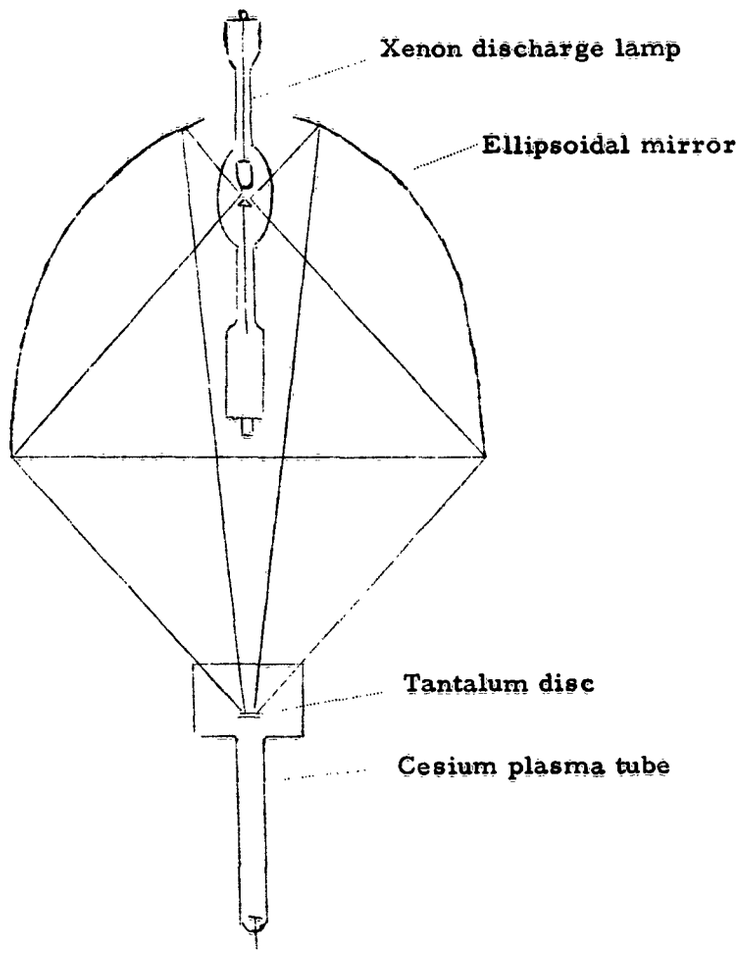

Fig. 13.

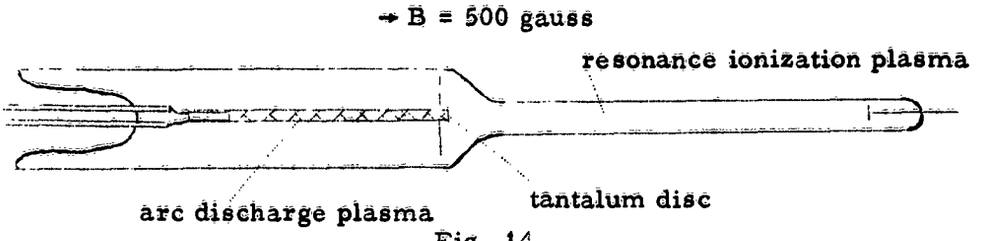

Fig. 14

In the second method we used an arc-discharge plasma with the tantalum disc as anod in order to heat the disc (Fig. 14). The cesium was held at a temperature of about 100°C. We measured a temperature of 2000°C with an arc-discharge current of 2-3 Amp. and a voltage of 30-40 Volts. The cathode in the arc-discharge, however, was not properly designed for such high currents and should be of a different type to stand this high current for a longer time.

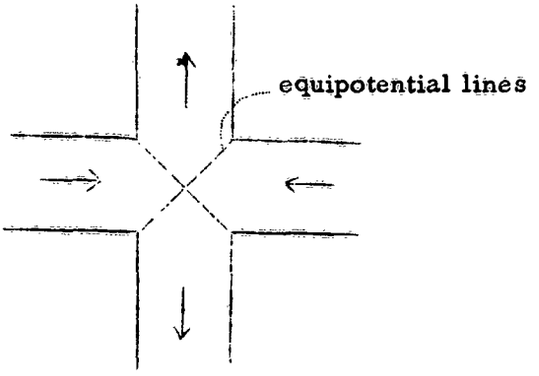

Fig. 15.

If current is sent through a thin metal cross (made of tungsten) as indicated in Fig. 15, the equipotential lines will be as shown by the dotted lines in Fig. 15. Thus, if a tantalum disc is fastened on equipotential lines no currents will flow in it and no potential gradients can develop across the disc. The heat conduction from the cross to the disc will, however, be quite good. A shield was put around the tungsten cross in order to shield the plasma created at the tungsten surface. We have measured a temperature on the disc of 2000°C. The highest voltage between two points on the disc was measured to be some microvolts. The magnetic field just outside the disc was maximum 5 gauss.

This device seems very promising and is now being built in a plasma tube.

2.6. A coil system, giving a magnetic field with high homogeneity

When studying wave propagation in plasmas, it is often necessary to have a magnetic field of a certain length with an extremely high homogeneity. For example in region 4 in the $(\frac{\omega_e}{\omega})^2-(\frac{\omega_c}{\omega})^2$ diagram (See section 2.1), a variation in the magnetic field of 1% could cause a change in phase velocity of the slow waves of 10% or more. To obtain a magnetic field of high homogeneity we have used a system consisting of four coils placed as in Fig. 16.

The field was calculated with the aid of a computer. The coil system gives a maximum field strength of 2500 gauss with a current of 45 Amp. The variation of the axial field component along the axis is plotted in Fig. 17. This shows a variation of less than 0,1% along 27 cm of the axis.

By proper adjustment of the coils it is possible to obtain a variation of less than 0.01% along 15 cm of the axis. The flexibility of the system also makes it possible to obtain fields of various shapes.

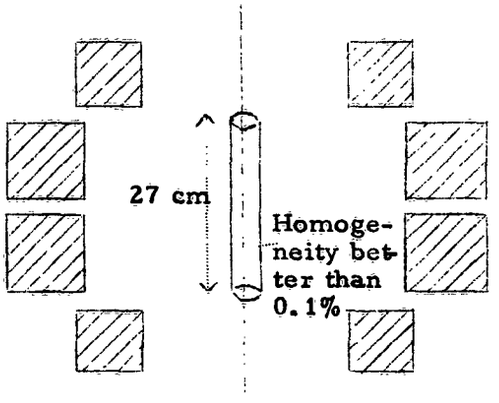

Fig. 16

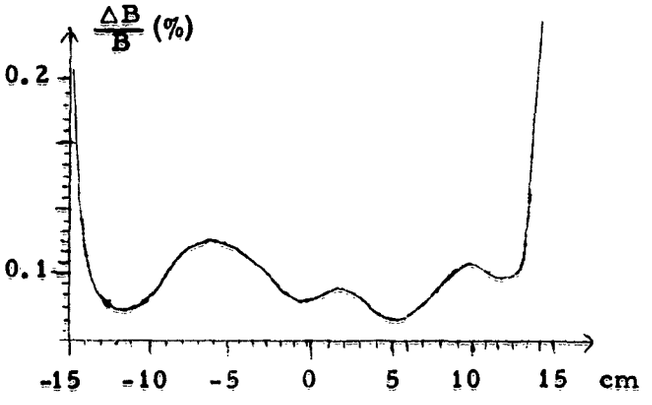

Fig. 17.

3. PLASMA RESONANCE IN SEMICONDUCTORS

At microwave frequencies the dielectric properties of a semiconductor are determined by two mechanisms: one is vibration of electrons captured at crystal lattice points or at impurity atoms, and the other is the convection current from free electrons and free positive "holes". The dielectric constant of the semiconductor thus contains one constant contribution from vibrations and one contribution from convection currents. The dielectric constant for a negatively doped semiconductor is

$$\varepsilon_3 = \varepsilon - \frac{e^2 n/\varepsilon_0 m^*}{(\omega^2 - j\frac{\omega}{\tau})}$$

where

- ε is the constant contribution from vibrating electrons,
- n is the density of conduction electrons,
- τ is the relaxation time of conduction electrons,
- m^* is the effective mass of conduction electrons.

m^* can have a value different from the free electron mass, because of the periodic force field in the crystal. When there is no static magnetic field, we get an isotropic dielectric constant for crystals of cubic symmetri, in spite of the structural anisotropy of the crystal. τ is a function of the temperature and of the degree of doping and of lattice imperfection.

As $\mathrm{Re}(\varepsilon_3)$ can take all values $< \varepsilon$, when n or ω varies, the requirements for plasma resonance effects are fullfilled, if the damping is small enough, i.e. τ is large enough. We have investigated plasma resonance in a semiconducting rod crossing a rectangular waveguide at right angles to the electric field lines.

THEORY

The configuration investigated is shown in Fig. 18.

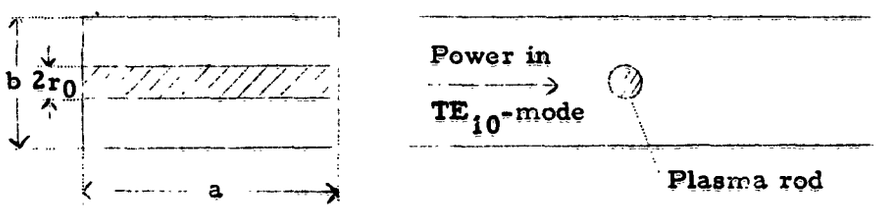

Fig. 18.

With the restrictions mentioned below one can show that this arrangement is described by the equivalent circuit in Fig. 19.

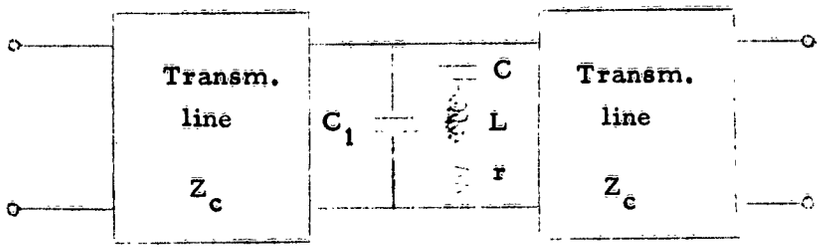

Fig. 19.

$$C_1 = \frac{\varepsilon - 1}{\varepsilon + 1} \cdot \frac{\varepsilon_0 \pi a r_0^2}{b^2}$$

$$C = \frac{2}{\varepsilon + 1} \cdot \frac{\varepsilon_0 \pi a r_0^2}{b^2}$$

$$L = \frac{(\varepsilon + 1)^2}{2\omega_p^2} \cdot \frac{b^2}{\varepsilon_0 \pi a r_0^2}$$

$$r = \frac{(\varepsilon + 1)^2}{2\omega_p^2 \tau} \cdot \frac{b^2}{\varepsilon_0 a r_0^2}$$

$$Z_c = \frac{2b}{a} \cdot \frac{\sqrt{\mu_0/\varepsilon_0}}{\sqrt{1 - (\lambda/2a)^2}}$$

where λ = free space wave-length.

$\omega_p^2 = \frac{e^2 n}{\varepsilon_0 m^*}$ = plasma frequency squared.

Z_c = characteristic impedance of the transmission line.

In C_1 flows the displacement current due to vibrating lattice electrons. In the series resonance circuit C, L, r, flows a convection current of free electrons (holes) parallel to the current in C_1. Both these currents shunt the transmission line. There are thus two different resonances in the system: one series resonance $\omega_1 = \sqrt{1/LC}$, giving a high shunt current and a reflection maximum, and one parallel resonance $\omega_2 = \sqrt{(C + C_1)/LCC_1}$ with $\omega_2 > \omega_1$, giving a low shunt current and a reflection minimum.

Expressed in physical quantities we get:

$$(\omega_p/\omega_1)^2 = (\varepsilon + 1) \qquad (\omega_p/\omega_2)^2 = (\varepsilon - 1)$$

The validity range of this equivalent circuit is given by three conditions.

The first condition is that the rod diameter is small compared to the free wave-length.

$$(\frac{2\pi r_0}{\lambda})^2 \ll 1$$

The second condition is that the rod diameter is small compared to the wave-length in the rod (or the skin depth).

$$|\varepsilon_3| \ (\frac{2\pi r_0}{\lambda})^2 \ll 1$$

The third condition ascertains that only the dipole type of field (not e.g. the quadrupole) contributes to the damping at the series resonance.

$$(\frac{2\pi r_0}{\lambda})^2 < \frac{2(g+1)}{\pi(\omega\tau)}$$

EXPERIMENTAL CONSIDERATIONS

For plasma resonance observations in semiconductors it is imperative to chose the semiconducting material and the experimental conditions carefully in order to have an $(\omega\tau)$-value as high as possible. As ω and ω_p are coupled by the resonance condition, a high ω means a low resistivity semiconductor, which in turn means a short relaxation time for electrons. A decrease in the temperature will increase τ, but at the same time the density, n, will decrease. All effects considered, the choice was made to take a Ge-rod, n-doped to have a room temperature resistivity of 6.55 Ω cm, and put it in an 8 mm waveguide at liquid hydrogen temperature. This gives an $(\omega\tau)$-value of about 3. An analysis shows, that the reflection coefficient from such a rod is almost unaffected by the passage through plasma resonance. Therefore it was chosen to observe the absorption resonance, which remains pronounced down to $\omega\tau = 2$. Rather than by varying the frequency, ω, the passage through resonance was made by varying the plasma frequency. The density, n, covers about three octaves, when the temperature is changed from the triple point to the boiling point of liquid hydrogen (13.8°K to 20.4°K). This manner of changing the density of free electrons has further the advantage, that thermal equilibrium is conserved.

EXPERIMENTAL SET UP

The experimental set up is shown in Fig. 20:

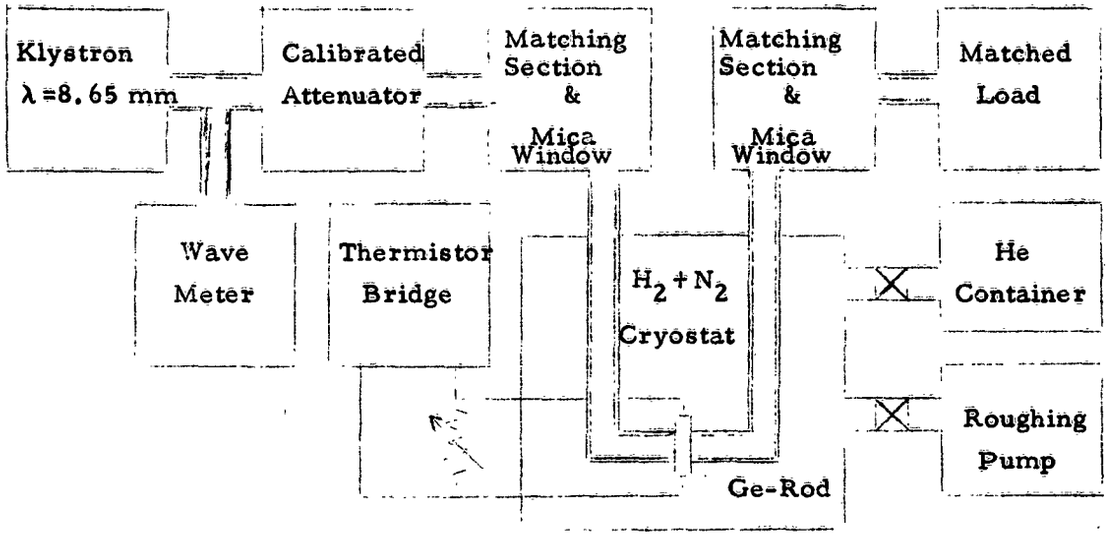

Fig. 20.

46 mW microwave power at λ = 8.65 mm wave-length is fed from a klystron through a calibrated attenuator to a Ge-rod of cross-section 0.45 x 0.60 mm. The circuit is terminated by a matched load and the section of waveguide in the cryostat is pressure isolated from the outside by means of individually matched mica windows.

The cryostat has an outer container with liquid nitrogen and an inner container with liquid hydrogen. The inner container can be evacuated above the hydrogen surface to lower the temperature and can be filled with helium gas to avoid air being sucked into the cryostat.

The Ge-rod, the resistance of which has a large negative temperature coefficient, is connected to a self-balancing thermistor bridge, which measures the microwave power absorbed by the rod. In order to vary the balanced resistance of the rod without changing the bridge resistance, we shunted the rod with a variable resistance. Knowing the shunt resistance, the power absorbed in the rod may easily be calculated from the reading of the power meter.

The bridge itself will thus keep the rod resistance constant and therefore also the density of free electrons. The surrounding hydrogen bath is kept on a temperature just below that of the rod. The calibrated attenuator is used to regulate the microwave power, so that the power meter of the thermistor bridge shows a relatively constant deflection, unaffected by variations in rod absorption.

MEASUREMENTS

As described above we measured the ratio of microwave power absorbed in the rod to power incident on the rod - the absorption coefficient - as a function of the rod resistance. The experimental points are shown in Fig. 21. The absorption coefficient shows the expected resonance behaviour.

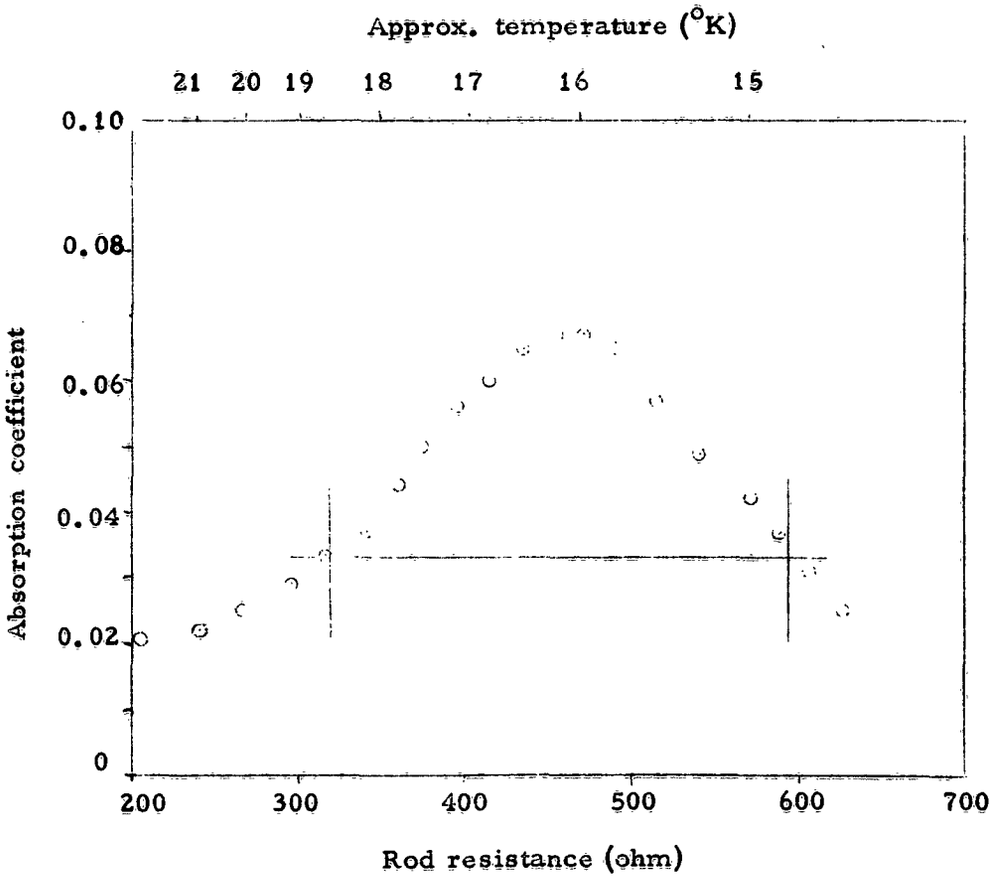

Fig. 21.

EVALUATION

From the dimensions of the rod (length: 11.2 mm, cross-section: 0.45 x 0.60 mm) we get a value for the product $(nR\mu)$, where R is rod resistance and μ is the carrier mobility of the rod:

$$(nR\mu) = 25.8 \cdot 10^{22} \quad \text{(MKSA)}$$

As $(\frac{\omega_r}{\omega})^2 = \frac{e^2 n}{\varepsilon_0 m^* \omega^2}$ and $m^* = 0.120\ m$ for Ge

We get

$$(\frac{\omega_p}{\omega})^2 = \frac{1.45 \cdot 10^5}{R\mu}$$

An analysis of the equivalent circuit in Fig. 2 shows, that the absorption maximum occurs for:

$$(\frac{\omega_p}{\omega})^2 \approx (\varepsilon + 1)\sqrt{1 + \frac{1}{(\omega\tau)^2}}$$

With $\varepsilon = 16$ for Ge and using $\mu = \frac{e\tau}{m^*}$

$$\omega\tau = \sqrt{(\frac{1265}{R_{res}})^2 - 1}$$

$R_{res} = 465\ \Omega$ from Fig. 4 gives $(\omega\tau)_{res} = 2.53$. This in turn gives us a value for the mobility of this Ge specimen at the temperature for resonance:

$$\mu_{res} = 17.0\ m^2/V \cdot sec$$

The carrier density can also be determined:

$$n_{res} = 3.26 \cdot 10^{19}\ m^{-3}$$

These values are in excellent agreement with Hall-effect determinations of the mobility in similar Ge samples (Debye and Conwell, Phys. Rev., 93, 693 (1954).

Assuming for the moment that $(\omega\tau)$ is a constant over the temperature range considered, we calculate the Q-value of the resonance:

$$Q = \frac{2(\omega_p/\omega)^2_{res}}{(\omega_p/\omega)^2_2 - (\omega_p/\omega)^2_1} = \frac{2/R_{res}}{(1/R_2 - 1/R_1)}$$

where index 1 and index 2 are related to the points, where the absorption has half its maximum value. From the equivalent circuit we get:

$$\frac{1}{Q} \approx \sqrt{\frac{4(\omega\tau)^2 + 3 - 4\omega\tau\sqrt{1 + (\omega\tau)^2}}{1 + (\omega\tau)^2}}$$

Solving the expression for $\omega\tau$ gives

$$\frac{1}{(\omega\tau)^2} = \frac{7/Q^2 + 4\sqrt{1 + 1/Q^2} - 4 - 1/Q^4}{(3 - 1/Q^2)^2}$$

with $R_2 = 320\ \Omega$ and $R_1 = 595\ \Omega$ from Fig. 4 we get

$$\frac{1}{Q} = 0.335$$

and hence $\omega\tau = 2.89$ from the resonance width.

Finally we consider the value of the maximum for the absorption A. We put

$$A^{(0)} = \frac{(\lambda/b)(2\pi r_0/\lambda)^2}{(\varepsilon + 1)\sqrt{1 - (\lambda/2a)^2}\left(\sqrt{1 + (\omega\tau)^2} - \omega\tau\right)}$$

(a = 7.1 mm and b = 3.55 mm) and get

$$A_{max} = \frac{A^{(0)}}{(1 + A^{(0)}/2)^2} = 0.067 \text{ from Fig. 21.}$$

It is now possible to calculate an equivalent radius r_0 for the rod putting 1) $\omega\tau = 2.53$ and 2) $\omega\tau = 2.89$:

1) $2r_0 = 0.76$ mm 2) $2r_0 = 0.71$ mm

Compared to the physical dimensions $2r_0 = 0.71$ mm will look as in Fig. 22:

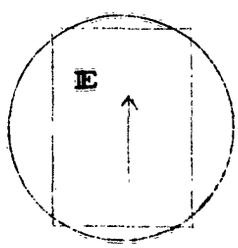

Fig. 22.

It should be observed, that the equivalent circuit of Fig. 19 will not describe the part of the absorption curve in Fig. 21 that falls below 350 Ω in an accurate way, as the skin depth is of the order of the diameter or less.

REFERENCES

1. B. Agdur et al: Scattering, Absorption and Emission of Light by Thin Metal Wires. To be published.

2. B. Agdur: Notes on the Propagation of Guided Microwaves through an Electron Gas in the Presence of a Static Magnetic Field.
Proc. of the Symposium on Electronic Waveguides, Polytechnic Inst. of Brooklyn, 1958.

3. A. W. Trivelpiece and R. W. Gould, Space Charge Waves in Cylindrical Plasma Columns.
J. Appl. Phys. 30, 1784 (1959).

ROYAL INST. OF TECHN.
STOCKHOLM, SWEDEN
MICROWAVE DEPT.
15 Dec. 1962

AF61 (052) 552
TR-1
MICROWAVE
ELECTRONICS

INTERACTION BETWEEN MICROWAVES AND PLASMAS IN GASDISCHARGES AND SEMICONDUCTORS

B. AGDUR

ABSTRACT: This summary report describes theoretical and experimental investigations of wave propagation in cylindrical plasma columns and plasma resonance phenomenon in semiconductors.

ROYAL INST. OF TECHN.
STOCKHOLM, SWEDEN
MICROWAVE DEPT.
15 Dec. 1962

AF61 (052) 552
TR-1
MICROWAVE
ELECTRONICS

INTERACTION BETWEEN MICROWAVES AND PLASMAS IN GASDISCHARGES AND SEMICONDUCTORS

B. AGDUR

ABSTRACT: This summary report describes theoretical and experimental investigations of wave propagation in cylindrical plasma columns and plasma resonance phenomenon in semiconductors.

ROYAL INST. OF TECHN.
STOCKHOLM, SWEDEN
MICROWAVE DEPT.
15 Dec. 1962

AF61 (052) 552
TR-1
MICROWAVE
ELECTRONICS

INTERACTION BETWEEN MICROWAVES AND PLASMAS IN GASDISCHARGES AND SEMICONDUCTORS

B. AGDUR

ABSTRACT: This summary report describes theoretical and experimental investigations of wave propagation in cylindrical plasma columns and plasma resonance phenomenon in semiconductors.

ROYAL INST. OF TECHN.
STOCKHOLM, SWEDEN
MICROWAVE DEPT.
15 Dec. 1962

AF61 (052) 552
TR-1
MICROWAVE
ELECTRONICS

INTERACTION BETWEEN MICROWAVES AND PLASMAS IN GASDISCHARGES AND SEMICONDUCTORS

B. AGDUR

ABSTRACT: This summary report describes theoretical and experimental investigations of wave propagation in cylindrical plasma columns and plasma resonance phenomenon in semiconductors.